photonics

Communication

Intra-Cavity Raman Laser Operating at 1193 nm Based on Graded-Index Fiber

Chunhua Hu [1,2] and Ping Sun [1,*]

[1] Shandong Provincial Engineering and Technical Center of Light Manipulations & Shandong Provincial Key Laboratory, School of Physics and Electronics, Shandong Normal University, Jinan 250014, China
[2] Electrical Engineering College, Binzhou University, Binzhou 256603, China
* Correspondence: sunping@sdnu.edu.cn

Abstract: Nonlinear Raman frequency conversion is an important technical scheme to obtain special optical band lasers based on conventional ion-doped lasers. In our work, we designed an intra-cavity Raman fiber laser based on graded index fiber (GRIF) as the Raman gain medium. Based on the fundamental-frequency 1080-nanometer laser, efficient first-order and second-order Stokes Raman lasers were obtained, respectively. When the power of the fundamental-frequency 1080-nanometer laser was 33.4 W, the output power of the second-order 1193-nanometer laser was 11.39 W. The corresponding conversion efficiency was 34.1%. To our knowledge, this is the first report of a second-order Raman output based on a GRIF and intra-cavity structure. In the experiment, the spectrum-purification process with the increase in power was also observed. Our experimental results prove that the intracavity Raman-laser system based on graded index fiber with a high optical conversion efficiency has important application potential for obtaining new special-application bands.

Keywords: Raman fiber laser; intra-cavity structure; graded index fiber; spectrum purification

check for updates

Citation: Hu, C.; Sun, P. Intra-Cavity Raman Laser Operating at 1193 nm Based on Graded-Index Fiber. *Photonics* **2023**, *10*, 33. https://doi.org/10.3390/photonics10010033

Received: 11 November 2022
Revised: 2 December 2022
Accepted: 21 December 2022
Published: 28 December 2022

1. Introduction

Lasers are new and innovative tools and are widely used in various industries [1–3]. In particular, fiber lasers have good heat-dissipation effects and pure flexible fiber structures. Therefore, fiber lasers have the advantages of compact structures, high output power and good beam quality, which is the focus of laser research at present [2–7]. Generally speaking, fiber lasers are mainly based on fibers doped with rare-earth ions as the gain medium to obtain the laser output. For example, the most commonly used Yb-doped fiber is used for 1010–1120 nm [2–6]. However, lasers based on ion-doped fibers are limited to obtaining specific wavelengths uncovered by doped-ion radiation bands. Nonlinear-frequency conversion technologies, such as frequency doubling [8,9], optical parametric oscillation [10,11], the Raman effect [12–17], etc., are effective means of performing new-wavelength-band laser operations. In particular, the Raman effect does not require phase matching and its own beam purification is the most commonly used nonlinear-frequency conversion technology in fiber lasers [12–17].

Previously, Raman gain media such as single-mode fibers [12,13], multi-mode fibers [14,15], Raman fibers (high-Raman-gain fibers) [16,17] and graded-index fibers [18–22] were commonly used to obtain Raman-laser output. In particular, the graded-index fiber has multiple advantages. Compared with the single-mode fiber, it does not require high beam quality from the fundamental frequency light. Because it has a larger limited area of light, its coupling efficiency is higher and its output power is larger [18,21]. Compared with specially designed Raman fibers, not only does it offer the advantages mentioned above, but, furthermore, its cost can be effectively controlled [18–22]. In addition, Raman lasers based on graded index fibers exhibit obvious beam-purification effects, which are intrinsic properties of graded-index multi-mode fibers due to their specially designed refractive-index-graded fiber cores. Through the Kerr effect [23–25] or stimulated scattering process, such as Raman or Brillouin scattering effects [16,26–28], spatial-beam purification can lead to high-quality beam output from multi-mode fibers pumped by multi-mode lasers with low beam quality [29], and can even achieve near-single-mode laser output [22].

Important advances have been made in the research on Raman lasers based on graded-index fibers. For example, Professor Babin's research group focuses on the research into GRIF Raman fibers pumped by basic multi-mode semiconductor lasers. In 2017, a high-power, high-efficiency graded-index-fiber Raman laser pumped by laser diode modules at 978 nm was demonstrated. A CW output power of 154 W was obtained at a wavelength of 1023 nm with an optical-to-optical conversion efficiency of 65%, making it the highest-power and highest-efficiency Raman fiber laser demonstrated in any configuration allowing brightness enhancement [18]. In 2019, A 976-nanometer all-fiber Raman laser enabling high beam quality with at direct multimode-laser diode pumping with low beam quality was demonstrated. The laser was applied in a 100/140 graded-index fiber with special in-fiber Bragg gratings that secured the generation of the Stokes beam with relatively good quality and high slope efficiency [19]. In addition, the frequency doubling of a multimode-diode-pumped GRIN-fiber Raman laser with improved beam quality in a simple single-pass scheme with a 5-mm PPLN crystal was studied. An efficient conversion into the blue spectral range with an output power of about 0.4 W@488 nm and 0.64 W@477 nm was demonstrated [20]. Furthermore, the power scaling in a high-power continuous-wave Raman fiber amplifier employing a graded-index passive fiber was reported by Chen et al. The maximum output power reached 2.087 kW at 1130 nm [21]. Fan et al. demonstrated a high-power Raman fiber amplifier with excellent beam quality based on graded-index fiber; the beam-quality factor M^2 at maximum output power was 1.6, with a brightness-enhancement factor of 27 [22]. It is obvious that at present, Raman lasers based on graded-index fibers mainly adopt the mode of extra-cavity Raman. In the extra-cavity structure, reflection grating, wavelength division multiplexer (WDM), or isolators working at the wavelengths of pump power and Stokes waves are usually used to separate the laser cavities of the pump laser and the Raman laser. However, there is no similar device between the pump laser and the Raman laser in the intra-cavity structure, and they share a common cavity [30]. Compared with the extra-cavity Raman laser, the intra-cavity Raman laser has a high power density and a low Raman-laser threshold because the fundamental-frequency light and the Raman light share a laser resonator. However, at present, there are relatively few reports on the intra-cavity Raman fiber laser based on the graded-index fiber. Furthermore, the intra-cavity Raman laser built in our work includes the advantages of the random Raman fiber laser (RRFL). Instead of using grating pairs, the naturally present Random distributed feedback from the 3.1-km GRIF is the main mechanism for cascade Raman shifts [31,32]. This can not only reduce the complexity, improve the compactness of the laser cavity and reduce costs, but also absorb the properties of RRFL-like time-domain stability, low coherence, and low noise [33–35].

In our work, we designed an intra-cavity second-order Raman fiber laser based on a 1080-nanometer Yb-doped fiber laser as the fundamental-frequency light and 105/125 graded-index fiber as the Raman gain medium, which was used to obtain a 1200-nanometer fiber laser. This 1200-nanometer laser has important applications in many biological fields and can be used as an excitation-light source to achieve fluorescence near the second near-infrared region in relevant research [36,37]. When the power of the 1080-nanometer laser is 33.4 W, the maximum second-order Raman output power reaches 11.39 W, and the corresponding fundamental Raman conversion efficiency is 34.1%. In addition, the purification process of the Raman laser spectrum with the increase in power was clearly observed in the experiment.

2. Experimental Setup

Figure 1 shows the construction of the Raman laser based on the graded-index fiber, in which two 30-watt 915-nanometer semiconductor lasers were used as pump sources. The pump light entered a 30-m 10/130 Yb-doped fiber through a (2 + 1) × 1 pump-beam combiner. The Yb-doped fiber was used to operate the fundamental-frequency laser. The signal end of the pump-beam combiner was sequentially fused with a 1080-nanometer high-reflection grating (99.9% reflectivity at 1080 nm) and a 50/50 coupler. The high-reflection grating can select the wavelength of fundamental-frequency light and reflect it in the manner of a total-reflection mirror. Furthermore, the Raman optical resonators can be formed under the naturally present random Rayleigh scattering as random distributed feedback (RDFB) along the 3.1-km GRIF and the broadband-reflective effect of Sagnac loop. A 3.1-km section of graded-index fiber (from YOFC) was used as the Raman gain medium. The end face of the fiber was perpendicularly cleaved. The whole laser was placed on a water-cooled plate with a set temperature of 20 °C in order to ensure the stability of the laser during high-power operation. The parameters of the output laser were analyzed by optical fiber spectrum analyzer, power meter, etc.

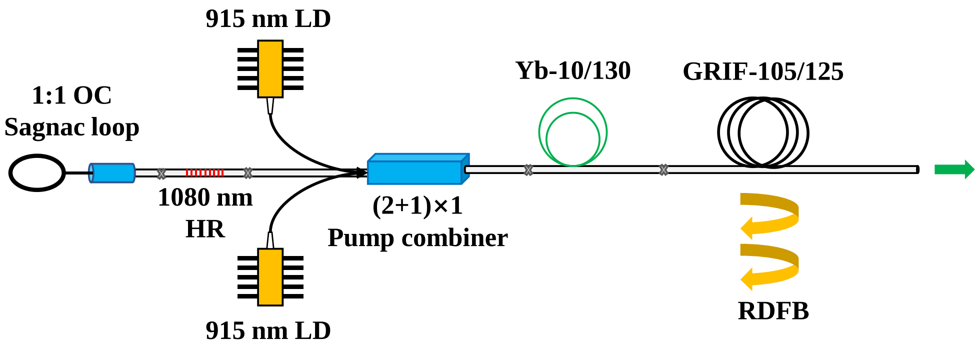

Figure 1. Schematic diagram of the intra-cavity Raman fiber laser.

3. Experimental Results and Discussion

In the experiment, without the Raman gain fiber, we first studied the output characteristics of the 1080-nanometer fundamental-frequency light. Figure 2a shows the relationship between the pump power and the output power. As shown in the figure, with the increase in the pump power, the output power also showed a linear increase and the slope of the linear fitting curve was 63%. When the pump power was 52.3 W, the maximum output power was 33.4 W and the corresponding optical-to-optical conversion efficiency and slope efficiency were 63.9% and 64.6% respectively. Figure 2b shows the emission spectrum of the laser. The center wavelength and 3-decibel bandwidth of the laser were 1079.92 and 1.04 nm, respectively.

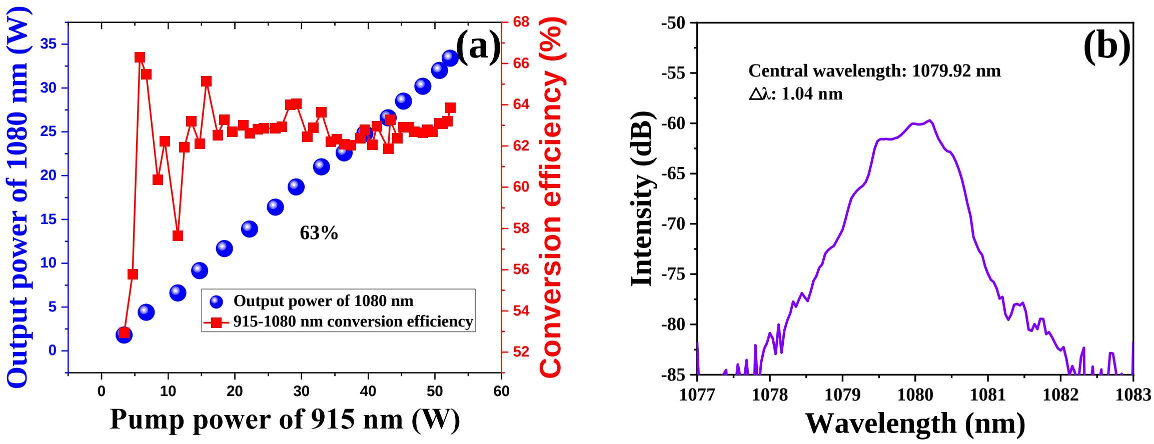

Figure 2. (**a**) Output power and conversion efficiency of the 1080-nanometer laser. (**b**) The emission optical spectrum of the 1080-nanometer laser.

Next, the 3.1-km graded-index fiber was added to the laser cavity to obtain the Raman laser output. Figure 3a shows the output power of the Raman laser versus the 1080-nanometer fundamental laser. The red line represents the linear fitting curve, which had a slope of 34.95%. The Raman laser's output characteristics were as follows. First, there was no Raman laser output when the input power of the 1080-nanometer fundamental-frequency laser was lower than 6.6 W. However, when the optical power of the fundamental frequency exceeded about 7 W, the first-order Raman laser, which operated at 1133 nm, began to appear. Additionally, the intensity of the first-order Raman laser gradually increased with the increase in the pump power. At the same time, due to the increase in the first-order Raman, the fundamental-frequency optical power began to decrease and the maximum power of the first-order Raman laser was about 6 W. Furthermore, when the first-order Raman laser was greater than 6 W, the second-order Raman light began to appear. Similarly, because the second-order Raman laser consumed the first-order Raman, the first-order Raman power gradually decreased and the second-order Raman-laser output power gradually increased with the increase in the pump power. The maximum output power of the second-order Raman was 11.39 W, corresponding to the optical-to-optical conversion efficiency of the fundamental to the Raman, which was 34.1%. The maximum output power was limited by the maximum pump power. No output from the third-order Raman laser was found in the experiment, limited by both the length of the GRIF and the maximum pump power.

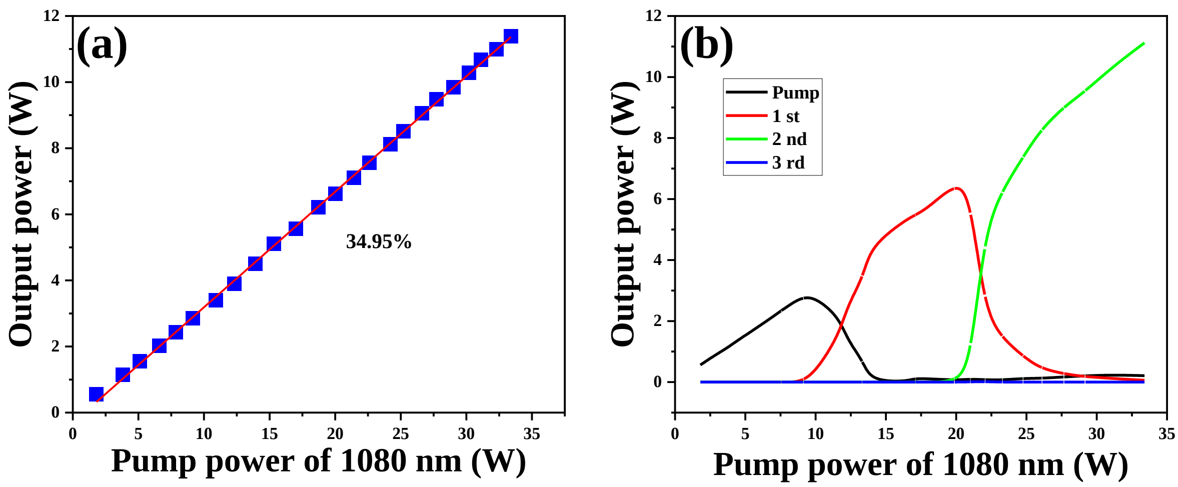

Figure 3. (**a**) Output power of the Raman laser versus the 1080-nanometer fundamental laser. (**b**) The evolution of Raman laser.

Figure 4 shows the spectrum-evolution process under different levels of 1080-nanometer fundamental-frequency power. As shown in the figure, with the increase in fundamental-frequency power, the number of Raman light orders increased significantly, after which the power of the higher-order Raman light gradually increased. The energy consumption of the lower-order Raman light took place at the same time. The output of the third-order and higher-order Raman laser was not observed in the experiment, mainly due to the limitation of the pump power and the Raman-gain fiber length described above.

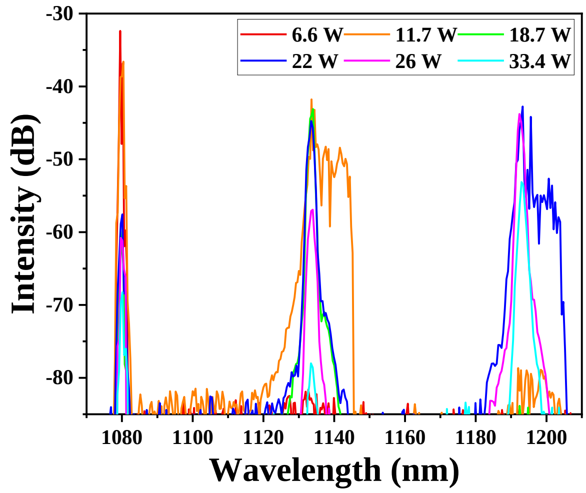

Figure 4. Spectrum evolution process under different powers of 1080-nanometer laser.

Figure 5 shows the changes in the first- and second-order Raman spectra under different power levels. As shown in Figure 5a, for the first-order Raman, the contrast of the Raman spectrum was low at low power. The same applied to the second-order Raman. When the second-order Raman appeared, the contrast of the Raman spectrum was also low. With the increase in power, the contrast of the Raman spectrum increased. In our opinion, this phenomenon was due to the beam-purification effect of the nonlinear Raman process.

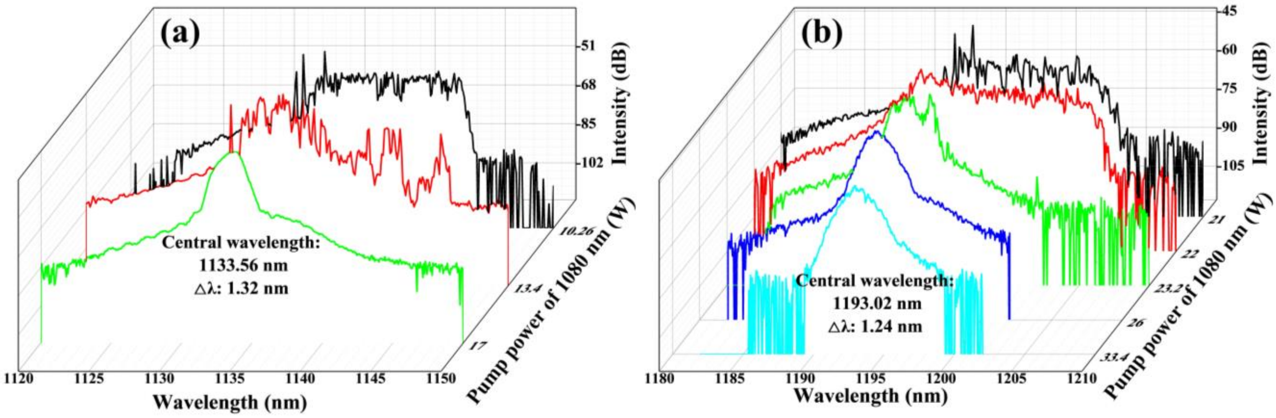

Figure 5. (**a**) The evolution of 1133-nanometer first-order Raman laser. (**b**) The evolution of 1193-nanometer second-order Raman laser.

4. Conclusions

In conclusion, based on the graded-index fiber, we studied the output characteristics of the intracavity Raman fiber laser. A 3.1-km 105/125 graded-index fiber was used as the Raman-gain medium. First and second-order Raman-laser output were observed in the experiment. The central wavelength of the second-order Raman was 1193 nm, which has important application value in the fields of fluorescence presentation and two-photon absorption. When the power of the 1080-nanometer fundamental frequency was 33.4 W, the maximum output power of the second-order Raman laser was 11.39 W. The experimental results show that the intra-cavity Raman laser based on the graded-index fiber had significant application prospects for obtaining low-threshold and special-wavelength lasers.

Author Contributions: Conceptualization, C.H. and P.S.; methodology, C.H. and P.S.; investigation, C.H.; resources, P.S.; writing—original draft preparation, C.H.; writing—review and editing, P.S.; supervision, P.S.; project administration, P.S.; funding acquisition, P.S. All authors have read and agreed to the published version of the manuscript.

Funding: This research was funded by the National Natural Science Foundation of China (61975099).

Institutional Review Board Statement: Not applicable.

Informed Consent Statement: Not applicable.

Data Availability Statement: The data presented in this study are available upon reasonable request.

Acknowledgments: Authors would like to thank Wenfeng Wang, and Jinlong Xue for their useful help.

Conflicts of Interest: The authors declare no conflict of interest.

References

1. Fermann, M.E.; Hartl, I. Ultrafast fiber laser technology. *IEEE J. Sel. Top. Quantum Electron.* **2009**, *15*, 191–206. [CrossRef]
2. Jeong, Y.E.; Sahu, J.K.; Payne, D.A.; Nilsson, J. Ytterbium-doped large-core fiber laser with 1.36 kW continuous-wave output power. *Opt. Express* **2004**, *12*, 6088–6092. [CrossRef] [PubMed]
3. Zhu, J.J.; Zhou, P.; Ma, Y.X.; Xu, X.J.; Liu, Z.J. Power scaling analysis of tandem-pumped Yb-doped fiber lasers and amplifiers. *Opt. Express* **2011**, *19*, 18645–18654. [CrossRef] [PubMed]
4. Bednyakova, A.E.; Gorbunov, O.A.; Politko, M.O.; Kablukov, S.I.; Smirnov, S.V.; Churkin, D.V.; Fedoruk, M.P.; Babin, S.A. Generation dynamics of the narrowband Yb-doped fiber laser. *Opt. Express* **2013**, *21*, 8177–8182. [CrossRef] [PubMed]
5. Cabasse, A.; Ortaç, B.; Martel, G.; Hideur, A.; Limpert, J. Dissipative solitons in a passively mode-locked Er-doped fiber with strong normal dispersion. *Opt. Express* **2008**, *16*, 19322–19329. [CrossRef]
6. Kuhn, V.; Kracht, D.; Neumann, J.; Weßels, P. 67 W of output power from an Yb-free Er-doped fiber amplifier cladding pumped at 976 nm. *IEEE Photon. Technol. Lett.* **2011**, *23*, 432–434. [CrossRef]
7. Moulton, P.F.; Rines, G.A.; Slobodtchikov, E.V.; Wall, K.F.; Frith, G.; Samson, B.; Carter, A.L. Tm-doped fiber lasers: Fundamentals and power scaling. *IEEE J. Sel. Top. Quantum Electron.* **2009**, *15*, 85–92. [CrossRef]
8. Ast, S.; Nia, R.M.; Schönbeck, A.; Lastzka, N.; Steinlechner, J.; Eberle, T.; Mehmet, M.; Steinlechner, S.; Schnabel, R. High-efficiency frequency doubling of continuous-wave laser light. *Opt. Lett.* **2011**, *36*, 3467–3469. [CrossRef]
9. Negel, J.P.; Loescher, A.; Voss, A.; Bauer, D.; Sutter, D.; Killi, A.; Ahmed, M.A.; Graf, T. Ultrafast thin-disk multipass laser amplifier delivering 1.4 kW (4.7 mJ, 1030 nm) average power converted to 820 W at 515 nm and 234 W at 343 nm. *Opt. Express* **2015**, *23*, 21064–21077. [CrossRef]
10. Leindecker, N.; Marandi, A.; Byer, R.L.; Vodopyanov, K.L.; Jiang, J.; Hartl, I.; Fermann, M.; Schunemann, P.G. Octave-spanning ultrafast OPO with 2.6-6.1 μm instantaneous bandwidth pumped by femtosecond Tm-fiber laser. *Opt. Express* **2012**, *20*, 7046–7053. [CrossRef]
11. Wu, R.F.; Lai, K.S.; Wong, H.F.; Xie, W.J.; Lim, Y.L.; Lau, E. Multiwatt mid-IR output from a Nd: YALO laser pumped intracavity KTA OPO. *Opt. Express* **2001**, *8*, 694–698. [CrossRef] [PubMed]
12. Supradeepa, V.R.; Feng, Y.; Nicholson, J.W. Raman fiber lasers. *J. Opt.* **2017**, *19*, 023001. [CrossRef]
13. Nicholson, J.W.; Yan, M.F.; Wisk, P.; Fleming, J.; DiMarcello, F.; Monberg, E.; Taunay, T.; Headley, C.; DiGiovanni, D.J. Raman fiber laser with 81 W output power at 1480 nm. *Opt. Lett.* **2010**, *35*, 3069–3071. [CrossRef] [PubMed]
14. Supradeepa, V.R.; Nicholson, J.W. Power scaling of high-efficiency 1.5 μm cascaded Raman fiber lasers. *Opt. Lett.* **2013**, *38*, 2538–2541. [CrossRef]
15. Churin, D.; Olson, J.; Norwood, R.A.; Peyghambarian, N.; Kieu, K. High-power synchronously pumped femtosecond Raman fiber laser. *Opt. Lett.* **2015**, *40*, 2529–2532. [CrossRef]
16. Baek, S.H.; Roh, W.B. Single-mode Raman fiber laser based on a multimode fiber. *Opt. Lett.* **2004**, *29*, 153–155. [CrossRef]
17. Xiao, Q.; Yan, P.; Li, D.; Sun, J.; Wang, X.; Huang, Y.; Gong, M. Bidirectional pumped high power Raman fiber laser. *Opt. Express* **2016**, *24*, 6758–6768. [CrossRef]
18. Glick, Y.; Fromzel, V.; Zhang, J.; Ter-Gabrielyan, N.; Dubinskii, M. High-efficiency, 154 W CW, diode-pumped Raman fiber laser with brightness enhancement. *Appl. Opt.* **2017**, *56*, B97–B102. [CrossRef]
19. Kuznetsov, A.G.; Kablukov, S.I.; Wolf, A.A.; Nemov, I.N.; Tyrtyshnyy, V.A.; Myasnikov, D.V.; Babin, S.A. 976 nm all-fiber Raman laser with high beam quality at multimode laser diode pumping. *Laser Phys. Lett.* **2019**, *16*, 105102. [CrossRef]
20. Kuznetsov, A.G.; Evmenova, E.A.; Dontsova, E.I.; Kablukov, S.I.; Babin, S.A. Frequency doubling of multimode diode-pumped GRIN-fiber Raman lasers. *Opt. Express* **2019**, *27*, 34760–34768. [CrossRef]
21. Chen, Y.A.; Yao, T.F.; Huang, L.J.; Xiao, H.; Leng, J.Y.; Zhou, P. 2 kW high-efficiency Raman fiber amplifier based on passive fiber with dynamic analysis on beam cleanup and fluctuation. *Opt. Express* **2020**, *28*, 3495–3504. [CrossRef] [PubMed]
22. Fan, C.C.; Xiao, H.; Yao, T.F.; Xu, J.M.; Chen, Y.Z.; Leng, J.Y.; Zhou, P. Kilowatt level Raman amplifier based on 100 μm core diameter multimode GRIN fiber with M^2 = 1.6. *Opt. Lett.* **2021**, *46*, 3432–3435. [CrossRef] [PubMed]
23. Zlobina, E.A.; Kablukov, S.I.; Wolf, A.A.; Nemov, I.N.; Dostovalov, A.V.; Tyrtyshnyy, V.A.; Myasnikov, D.V.; Babin, S.A. Generating high-quality beam in a multimode LD-pumped all-fiber Raman laser. *Opt. Express* **2017**, *25*, 12581–12587. [CrossRef]
24. Lombard, L.; Brignon, A.; Huignard, J.P.; Lallier, E.; Georges, P. Beam cleanup in a self-aligned gradient-index Brillouin cavity for high-power multimode fiber amplifiers. *Opt. Lett.* **2006**, *31*, 158–160. [CrossRef] [PubMed]

25. Podivilov, E.V.; Kharenko, D.S.; Gonta, V.A.; Krupa, K.; Sidelnikov, O.S.; Turitsyn, S.; Fedoruk, M.P.; Babin, S.A.; Wabnitz, S. Hydrodynamic 2D turbulence and spatial beam condensation in multimode optical fibers. *Phys. Rev. Lett.* **2019**, *122*, 103902. [CrossRef] [PubMed]
26. Flusche, B.M.; Alley, T.G.; Russell, T.H.; Roh, W.B. Multi-port beam combination and cleanup in large multimode fiber using stimulated Raman scattering. *Opt. Express* **2006**, *14*, 11748–11755. [CrossRef] [PubMed]
27. Chiang, K.S. Stimulated Raman scattering in a multimode optical fiber: Evolution of modes in Stokes waves. *Opt. Lett.* **1992**, *17*, 352–354. [CrossRef]
28. Bruesselbach, H. Beam cleanup using stimulated Brillouin scattering in multimode fibers. In Proceedings of the Conference on Lasers and Electro-Optics, Baltimore, MD, USA, 2–7 May 1993; Optical Society of America: Washington, DC, USA, 1993; p. CThJ2.
29. Niang, A.; Modotto, D.; Tonello, A.; Mangini, F.; Minoni, U.; Zitelli, M.; Fabert, M.; Jima, M.A.; Egorova, O.N.; Levchenko, A.E.; et al. Spatial beam self-cleaning in tapered Yb-doped GRIN multimode fiber with decelerating nonlinearity. *arXiv* **2019**, arXiv:2001.00105. [CrossRef]
30. Wu, H.; Wang, Z.N.; He, Q.H.; Sun, W.; Rao, Y.J. Common-cavity ytterbium/Raman random distributed feedback fiber laser. *Laser Phys. Lett.* **2017**, *14*, 065101. [CrossRef]
31. Chen, L.J.; Song, R.; Lei, C.M.; Yang, W.Q.; Hou, J. Random fiber laser directly generates visible to near-infrared supercontinuum. *Opt. Express* **2019**, *27*, 29781–29788. [CrossRef]
32. Song, J.X.; Ren, S.; Liu, W.; Li, W.; Wu, H.; Ma, P.F.; Zhang, H.W.; Zhou, P. Temporally stable fiber amplifier pumped random distributed feedback Raman fiber laser with record output power. *Opt. Lett.* **2021**, *46*, 5031–5034. [CrossRef] [PubMed]
33. Turitsyn, S.K.; Babin, S.A.; El-Taher, A.E.; Harper, P.; Churkin, D.V.; Kablukov, S.I.; Ania-Castañón, J.D.; Karalekas, V.; Podivilov, E.V. Random distributed feedback fibre laser. *Nat. Photonics* **2010**, *4*, 231–235. [CrossRef]
34. Babin, S.A.; Vatnik, I.D.; Laptev, A.Y.; Bubnov, M.M.; Dianov, E.M. High-efficiency cascaded Raman fiber laser with random distributed feedback. *Opt. Express* **2014**, *22*, 24929–24934. [CrossRef] [PubMed]
35. Zhang, H.W.; Huang, L.; Song, J.X.; Wu, H.; Zhou, P.; Wang, X.L.; Wu, J.; Xu, J.M.; Wang, Z.N.; Xu, X.J.; et al. Quasi-kilowatt random fiber laser. *Opt. Lett.* **2019**, *44*, 2613–2616. [CrossRef]
36. Zhang, H.X.; Fan, Y.; Pei, P.; Sun, C.X.; Lu, L.F.; Zhang, F. Tm^{3+}-Sensitized NIR-II Fluorescent Nanocrystals for In Vivo Information Storage and Decoding. *Angew. Chem. Int. Ed.* **2019**, *58*, 10153–10157. [CrossRef] [PubMed]
37. Dou, K.; Feng, W.Q.; Fan, C.; Cao, Y.; Xiang, Y.H.; Liu, Z.H. Flexible designing strategy to construct activatable NIR-II fluorescent probes with emission maxima beyond 1200 nm. *Anal. Chem.* **2021**, *93*, 4006–4014. [CrossRef] [PubMed]